DEVELOPMENT OF ALGORITHMS FOR CLUSTER FINDING AND TRACK RECONSTRUCTION IN THE FORWARD MUON SPECTROMETER OF ALICE EXPERIMENT

A. Zinchenko*, G. Chabratova, V. Pismennaia, A. Vodopianov, JINR, Dubna, 141980, Russia
For the ALICE Collaboration

Abstract

A simultaneous track finding / fitting procedure based on Kalman filtering approach has been developed for the forward muon spectrometer of ALICE experiment.

In order to improve the performance of the method in high-background conditions of the heavy ion collisions the "canonical" Kalman filter has been modified and supplemented by a "smoother" part. It is shown that the resulting "extended" Kalman filter gives better tracking results and offers higher flexibility.

To further improve the tracking performance in a high occupancy environment a new algorithm for cluster / hit finding in cathode pad chambers of the muon spectrometer has been developed. It is based on the expectation maximization procedure for a shape deconvolution of overlapped clusters. It is demonstrated that the proposed method allows to reduce the loss of the coordinate reconstruction accuracy for high hit multiplicities and achieve better tracking results.

THE FORWARD MUON SPECTROMETER OF ALICE

A Large Ion Collider Experiment (ALICE) is the only detector dedicated to the study of nucleus-nucleus collisions at the LHC [1]. It will investigate the physics of strongly interacting matter at extreme energy densities, where the formation of a new phase of matter, the quark-gluon plasma (QGP) is expected. One of the most sensitive probes of the plasma is expected to be the production of heavy quark vector mesons, i.e. J/Ψ, Ψ', Υ, Υ', Υ'', which could be measured through their muonic decay in a forward muon arm.

The forward muon spectrometer (Fig. 1) consists of:

- a aront absorber which absorbs the hadrons and photons from the interaction vertex,
- a 10 plane tracking system with high granularity,
- a large area dipole magnet,
- a passive muon filter wall followed by four planes of trigger chambers.

Partially located inside the central magnet, the front absorber is designed to suppress as much as possible the high hadron flux. Outside the central magnet there is a large warm dipole magnet with a 3 Tm field integral. A total of ten cathode pad chambers grouped in five stations define the muon trajectories. A second absorber and four planes of resistive plate detectors are used for muon identification and triggering. The front absorber and the muon filter wall set the cut-off muon momentum at 4 GeV/c and the detectors cover the angular region between 2° and 9° in θ.

Despite the heavy shielding, for central Pb-Pb collisions, a few hundred particles should hit each chamber with a maximum hit density of 10^{-2} cm^{-2}. Cathode pad chambers have been chosen because they can be equipped with high granularity read-out and reach the required resolution which should be better than 100 μm. Two tracking stations are located in front of the dipole magnet, another one is located inside, and two more stations sit behind the magnet. Each station is made of two chamber planes and each chamber has two cathode planes which are both read in order to have a two-dimensional hit information. Each individual chamber has an average thickness below 3% of X_0. The chambers have a total surface of 100 m^2 and a total number of channels of about one million. This should give a maximum occupancy of 5% with the nominal rate defined above.

TRACK RECONSTRUCTION METHODS

"Traditional" Track Reconstruction Method

The "traditional" method [2] is based on the following approach: tracks start from segments (vectors) found in the last two tracking stations, where a segment is built from a pair of points from two chamber planes of the same tracking station. Then each track is extrapolated to the first station and segments or single hits found in the other stations are added. A track is validated if the algorithm finds at least 3 hits (out of 4 possible) in the detector planes behind the dipole magnet, at least 1 hit (out of 2) in the station located inside the magnet and 3 hits (out of 4) in the chambers before the magnet.

Kalman Filter

The Kalman filter [3],[4] is a set of mathematical equations that provides an efficient computational (recursive) solution of the least-squares method.

The tasks for charged-track reconstruction in experimental high-energy physics are pattern recognition (i.e. track finding) and track fitting. The Kalman filtering method provides a mean to do pattern recognition and track fitting si-

---

* Alexandre.Zintchenko@cern.ch

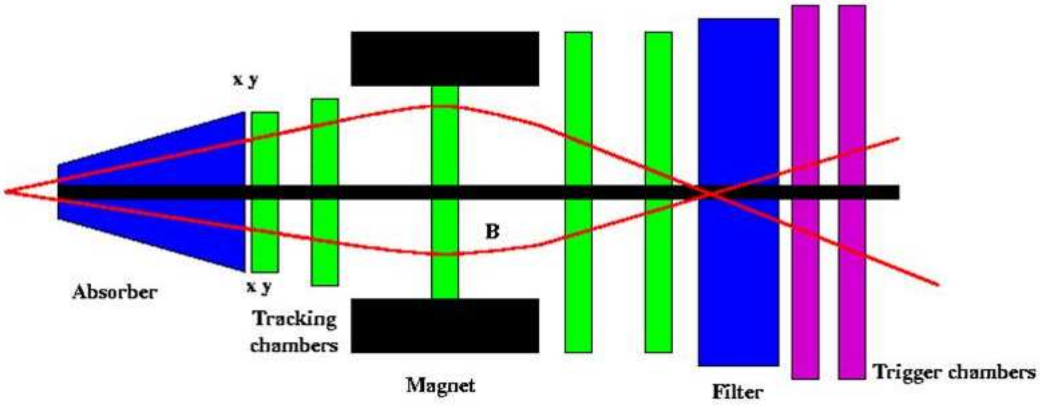

Figure 1: Schematic side view of the ALICE forward muon spectrometer.

multaneously. The multiple scattering can be handled properly by the method too.

The algorithm starts from track candidates (”seeds”), for which vectors of initial parameters and covariance matrices are evaluated. Then each track is propagated to some surface (detector or intermediate point). The new covariance matrix can be obtained using the Jacobian matrix of the transformation, i.e. the matrix of derivatives of propagated track parameters with respect to current parameters.

If there is a new measurement in a certain window around the extrapolated point with its vector of local measured parameters and covariance matrix it can be added to the track, and the Kalman filter updates the vector of parameters, covariance matrix and χ^2-value of the track.

Application to the Forward Muon Spectrometer

A Kalman track seed is created for all track segments found in detector stations 4 and 5 (as for the “traditional” method). Tracks are parameterized as $(y, x, \alpha, \beta, q/p)$, where y is a coordinate in the bending plane, x is a non-bending coordinate, α is a track angle in the bending plane with respect to the beam line, β is an angle between the track and the bending plane, q and p are the track charge and momentum, respectively.

A track starting from a seed is followed to the station 1 or until it is lost (if no hits in a station are found for this track) according to the following procedure. It propagates the track from the current z-position to a hit with the nearest z-coordinate. Then for given z it looks for the hits within certain window w around the transverse track position (the window is taken to be 4σ). After this there are two possibilities. The first one is to calculate the χ^2-contribution of each hit and consider the hit with the lowest contribution as belonging to the track. The second way is to use a so-called track branching and pick up all the hits inside the acceptance window. Efficiency and mass resolution tests have shown that the second way gives a better result and so is used in the current implementation.

Since the magnetic field is generally non-uniform, the Runge-Kutta algorithm is used for propagation of track parameters. Effect of the track chamber material is taken into account by adding a multiple scattering term to the track covariance matrix for each chamber traversed.

After propagation to the chamber 1 all tracks are sorted according to their quality, defined as

$$Quality = N_{hits} + \frac{\chi^2_{max} - \chi^2}{\chi^2_{max} + 1},$$

where χ^2_{max} is the maximum acceptable χ^2 of tracks. Then duplicated tracks are removed, where duplicated means having half or more of their hits shared with another track with a higher quality.

Smoother

The description of the smoother formalism can be found in [4]. Smoothing means the evaluation of track parameters at any point along the track after its reconstruction, i.e. using information from all the measured points belonging to the track. Thus, the smoother provides the most optimal conditions for a detection of wrongly assigned hits.

Given that the smoother procedure exists the following tracking strategy can be proposed. If the background conditions are heavy and result in loss of efficiency, the size of the window used to accept measurements during the direct track propagation should be increased. This allows to find track continuation in the detector geometry with large distances between consecutive measurements (up to 2.5 m in the muon spectrometer) even when the assumed measurement error is underestimated in some cases (as usually happens for overlapped clusters). Then the found track should be passed through the smoother in order to reject measurements with χ^2 above certain cut (outliers).

The price to pay for the smoother is the extra information to be kept for each point of the track candidate (vectors of extrapolated and filtered track parameters, extrapolated and filtered covariance matrices and propagation matrix) and additional processing time due to wider acceptance windows. However, since there are about 10 points per track in average, the amount of extra information is quite moderate. In addition, by changing two correlated parameters (acceptance window and χ^2-cut) it is possible to tune the

Table 1: Performance results of the “traditional” tracking method and Kalman filter. Background level is expressed in terms of the nominal background events. Mass resolution is taken from the fit to the Gaussian in the 0.5 GeV-range around peak position. Results for the extended Kalman filter are shown for two sets of parameters: “tight” muons with w and χ^2_{max} equal to 8σ and 25 and “loose” muons (in parentheses) with 12σ and 100.

	“Traditional” tracking			“Canonical” Kalman filter			“Extended” Kalman filter		
Background level	0	1	2	0	1	2	0	1	2
Single track efficiency, %	98.8	94.7	85.9	94.2	82.5	62.8	98.0 (98.9)	87.8 (93.5)	70.6 (83.6)
Υ mass resolution, MeV	95.3	108.4	153.6	89.9	98.3	111.0	90.7 (98.2)	95.3 (109.2)	107.2 (137.2)
CPU time/event, s	0.9	3.7	8.1	0.4	0.9	2.6	0.4 (0.4)	1.3 (1.4)	4.9 (7.6)

algorithm to have a high tracking efficiency with good track quality and reasonable CPU consumption.

Tracking Results

The results presented below were obtained for dimuons with θ = 2 - 9° from upsilon decays. The effect of the background was simulated by adding hits from HIJING [5] generated central events with 6000 charged particles per rapidity unit. Two such events added together made one so-called nominal background event. The merged (signal+background) events were processed with the tracking algorithms under study.

The tracking results for different background levels are summarized in Table 1 and Fig. 2. One can see, that for high background levels the “canonical” Kalman filter gives higher track quality (better mass resolution) than the “traditional” method at the expense of reduced track finding efficiency. It happens because of the local character of the Kalman filter. On the other hand, the smoother allows to find a way to approach the single track efficiency obtained in the “traditional” method having still higher track quality or to find a combination of parameters, which gives results satisfactory from the physics point of view.

APPLICATION OF THE EM ALGORITHM FOR CLUSTER FINDING IN CATHODE PAD CHAMBERS

The “traditional” cluster finding method is based on the model which can be briefly described as follows. The charge released by a charged track, passing through a chamber, induces signals on cathode pads. The pad charge distribution can be described by a two-dimensional integral of the Mathieson function [6]. Therefore, in case of a single track, its coordinates can be extracted from the fit of the pad charge distribution by a Mathieson function based expression. If there are several close tracks the number of fit parameters should be increased accordingly. The number of track candidates is estimated from the number of local maxima in the pad charge distribution.

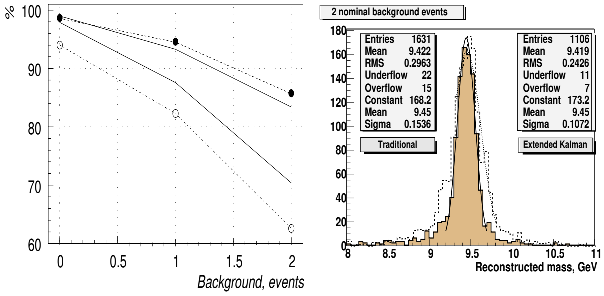

Figure 2: Left) Single track efficiency versus occupancy, expressed in terms of the number of added nominal background events. Closed circles - “traditional” tracking, open circles - “canonical” Kalman filter, band shows results for “extended” Kalman filter for different algorithm parameters. Right) Reconstructed dimuon invariant mass and fit to the Gaussian for the case of background level 2: hatched histogram and solid line after the extended Kalman filter and dashed histogram and dotted line after the traditional method.

As was mentioned above, the pad sizes of the cathode pad chambers have been selected according to the requirement to have an occupancy around 5%. For the first tracking station it corresponds to the minimum pad size of 4×6 mm^2. However, as was seen from simulation, the amount of events with significant overlapping of signal and background induced pad charges is not negligible for high background levels. For those cases the estimation of the number of track candidates from the local maxima is not sufficiently accurate and results in deterioration of coordinate resolution.

The proposed cluster finding algorithm is based on a Maximum Likelihood - Expectation Maximization (MLEM or EM) technique [7]. The essence of the method is that it iteratively solves the inverse problem of a signal deconvolution.

The algorithm starts from finding groups of adjacent pads on one cathode and overlapping with them pads on the other cathode which together form a “precluster”. For given precluster an array of pixels in the anode plane is built with the size defined by the overlap of pads on both cathodes. It is assumed that each pixel contains a track. If the initial value of energy release from a track j (i.e. pixel intensity) was q^0_j (usually all q^0_j’s are set to 1) then the fol-

Table 2: The same as in Table 1 for hits reconstructed with the new cluster finder. "Tight" muons with w = 4σ and χ^2_{max} = 25 and "loose" muons with 8σ and 100.

	"Traditional" tracking			"Canonical" Kalman filter			"Extended" Kalman filter		
Background level	0	1	2	0	1	2	0	1	2
Single track efficiency, %	98.9	97.8	95.7	97.3	93.7	89.2	98.7 (99.6)	97.2 (98.7)	95.0 (97.2)
Υ mass resolution, MeV	91.0	96.4	101.1	89.5	93.4	97.5	88.6 (92.4)	91.6 (98.6)	94.8 (99.3)
CPU time/event, s	0.7	3.6	8.2	0.4	1.0	3.3	0.4 (0.4)	1.3 (1.4)	4.3 (7.4)

lowing iterative procedure will update its value:

$$q_j^{k+1} = \frac{q_j^k}{\sum\limits_{i=1}^{N_{pads}} c_{ij}} \sum_{i=1}^{N_{pads}} c_{ij} \frac{Q_i}{f_i^k} \quad \text{with} \quad f_i^k = \sum_{j=1}^{N_{pix}} c_{ij} q_j^k,$$

where f_i^k is the expected signal on pad i if the pixel intensity was q_j^k (at the k^{th} iteration), Q_i is the measured signal on pad i, c_{ij} is the pixel-to-pad coupling (given by the Mathieson integral) and N_{pix} is the number of pixels in the array.

After several iterations (10-15) the larger pixel dimension is decreased by two and pixels with the lowest intensity are removed if the total number of pixels exceeds the number of pads. This is necessary in order to ensure the unique solution of the system. Then the iterative procedure is performed again. The algorithm stops when the pixel size becomes sufficiently small (1 mm) (see Fig. 3). After that, the resulting pixel clusters are used as fitting seeds for the fitting procedure.

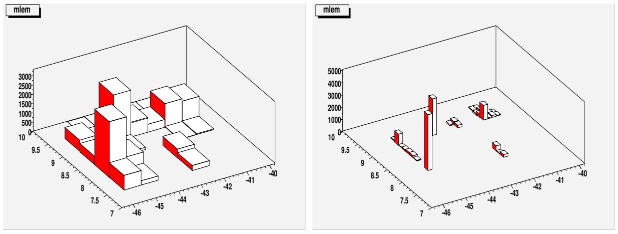

Figure 3: Distribution of pad charges on a single cathode (left) and pixel charge distribution after the last execution of the EM-based procedure (right).

Results for "New" Clusters

The coordinate residuals (a difference between the reconstructed and generated hit coordinates) in the bending plane for the "traditional" and EM-based cluster finding algorithms are presented in Fig. 4. The tracking results with hits found by the "new" cluster finding algorithm are summarized in Table 2 and Fig. 5. One can clearly see the improvement.

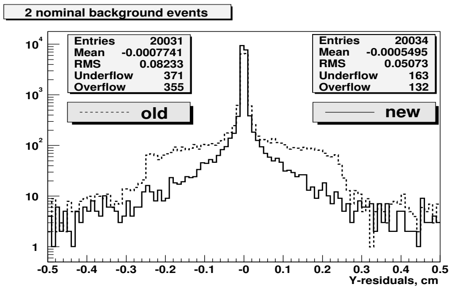

Figure 4: Coordinate residuals for the bending plane of cathode pad chambers.

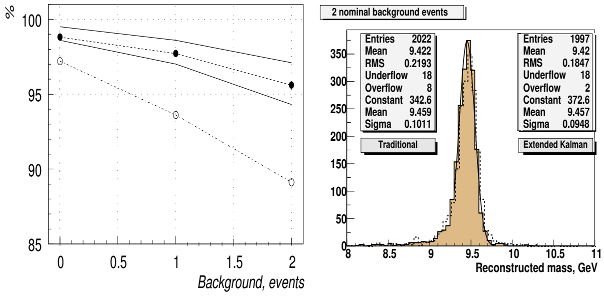

Figure 5: The same as in Fig. 2 for "new" clusters.

CONCLUSIONS

The results presented above allow to conclude that the extended Kalman filter (with a smoother) offers high flexibility and resistance against the background originated effects. The smoother part can help to overcome the tracking algorithm performance deterioration when the measurement quality is not maximized yet (hit finding algorithm is not optimal or detector alignment problems are not solved). On the other hand, once the problems are solved the smoother can be switched off to exclude some overhead resulting from its operation.

REFERENCES

[1] ALICE Collaboration, CERN/LHCC/95-71 (1995).

[2] ALICE Collaboration, CERN/LHCC/96-32 (1996).

[3] P. Billoir and Q. Qian, Nucl. Instr. and Meth. A294 (1990) 219.

[4] R. Fruhwirth, Nucl. Instr. and Meth. A262 (1987) 444.

[5] X.N. Wang and M. Gyulassy, Phys. Rev. D44 (1991) 3501.

[6] E. Mathieson, Nucl. Instr. and Meth. A270 (1988) 602.

[7] L.A. Shepp and Y. Vardi, IEEE Trans. Med. Imag. 1 (1982) 113.